SIMPLE SHAPE PARAMETER ESTIMATION FROM BLURRED OBSERVATIONS FOR A GENERALIZED GAUSSIAN MRF IMAGE PRIOR USED IN MAP IMAGE RESTORATION

Brian D. Jeffs and Wai Ho Pun
Department of Electrical and Computer Engineering, Brigham Young University
459 CB, Provo, UT 84602, USA. E-mail: bjeffs@ee.byu.edu

Abstract

The Generalized Gaussian Markov Random Field (GGMRF) is used as an image prior model in MAP restoration of blurred and noise corrupted images. This model is adapted to characteristics of the true image by jointly estimating the true image and the GGMRF shape parameter, p, from the corrupted observation. A simple estimator for p based on sample kurtosis is introduced. It is shown that the value of p ranges widely when modeling typical images and texture fields. Higher quality restorations can be obtained when the estimated p value is used, rather than commonly used arbitrary choices.

I. Introduction

In this paper we present a Bayesian approach to image restoration that uses the observed image data to control the form of the image prior model. The image is modeled using the Generalized Gauss Markov random field (GGMRF) [1], but unlike previous applications of this model to MAP restoration, we assume the image prior shape parameter, p, is unknown. Both the true image and p are estimated from the degraded observation. The proposed approach can yield better results than other Bayesian methods where the image prior is fixed arbitrarily. Such methods cannot adapt to the wide range of image structural forms regularly encountered in restoration applications.

MAP image restoration using the GGMRF prior with a fixed value of p was introduced by Bouman and Sauer and was shown to improve edge rendering [1]. Adaptive estimation of the shape parameter, p, during restoration was first presented by us in [2]. Saquib and Bouman have recently proposed excellent maximum likelihood estimators for p and the associated GGMRF scale parameter, T [3]. In their restoration simulations however, a fixed compromise value of $p = 1.1$ was used because of the belief that most images are best modeled with a $p \leq 1$, and because simple techniques for optimizing the image posterior distribution require $p > 1$, in order to insure a convex cost function.

We will show that for a GGMRF to accurately model a variety of image classes, p must be allowed to vary over a range of at least $0.3 \leq p \leq 2.6$. We also demonstrate successful joint estimation of p and the true image using only the blurred and noise corrupted observation. Restoration examples with $p < 1$, $p \approx 1$, and $p \approx 2$ will be discussed.

We adopt the following familiar linear observation model

$$\mathbf{y} = \mathbf{H}\mathbf{x} + \mathbf{n}, \tag{1}$$

where $\mathbf{y}$ is the row scanned degraded image vector, $\mathbf{H}$ is the convolutional blur matrix, $\mathbf{x}$ is the true image vector, and $\mathbf{n}$ is additive noise.

II. Image Prior Model

To model an image, $\mathbf{x}$, as a Markov random field (MRF), the prior distribution is usually specified through as a Gibb's distribution of the form [4]

$$f_x(\mathbf{x}) = \frac{1}{Z} e^{-\frac{1}{T}\sum_{c\in C} \phi_c(\mathbf{x})}, \tag{2}$$

where T is the scale parameter, $\phi_c(\cdot)$ is the potential function over clique c, and C is the set of all cliques defined for the neighborhood system of the Markov field.

The potential function for the first order symmetric GGMRF is $\phi(x_s, x_t; p) = |x_s - x_t|^p$ where s and t are nearest neighbor pixels which form the clique we will designate as $c = \langle s,t \rangle$ [1]. Figure 1 plots this potential for various values of p as a function of the neighboring pixel differences, $d_{s,t} = x_s - x_t$. The value of p determines significant structural features in $\mathbf{x}$. For synthetic GGMRF images, we have noted that small p values yield sharp edge transitions and constant valued regions, while large p (e.g. $p \geq 2$) produces smooth transitions between regions.

When a GGMRF is used to model actual images, the best fit for p varies over a wide range. Table I lists 34 images for which p values were estimated using the method described below in Section III. Note the wide variation for p. Figure 2 shows eight of these images. The complex scene images with sharp boundaries yield p values well below 1.0, while many texture-like fields have much higher corresponding p values.

0-7803-3258-X/96/$5.00 © 1996 IEEE

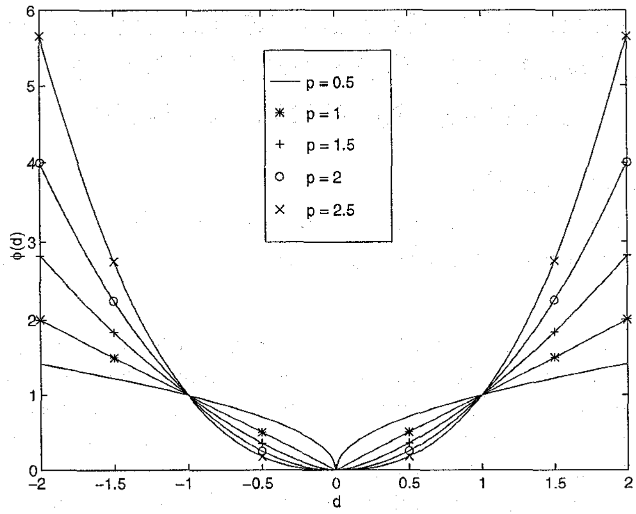

Fig. 1. Potential function of GGMRF for different values of p. Note that $x = d_{s,t}$ in this figure.

Adopting the first order GGMRF as our image prior model, the joint distribution for $\mathbf{x}$ is given by

$$f_x(\mathbf{x};p) \propto \exp\left\{-\left[\frac{A}{\sigma}\right]^p \sum_{(s,t)\in\mathcal{C}} |x_s - x_t|^p\right\}, p > 0 \quad (3)$$

where $A = \left[\frac{\Gamma(3/p)}{\Gamma(1/p)}\right]^{1/2}$ and σ is the standard deviation parameter.

Given an observed image $\mathbf{y}$, and assuming the additive noise is Gaussian, the adaptive MAP estimate of $\mathbf{x}$ is $\hat{\mathbf{x}} = \arg\{\min_{\mathbf{x},p} \Phi(\mathbf{x},\mathbf{y};p)\}$, where

$$\Phi(\mathbf{x},\mathbf{y};p) = \sum_{s\in S}[y_s - (\mathbf{H}\mathbf{x})_s]^2 + \gamma\left[\frac{A}{\sigma}\right]^p \sum_{(s,t)\in\mathcal{C}} \phi(x_s, x_t; p), \quad (4)$$

and $\mathcal{C}$ contains all nearest neighbor pairs, and S is the set of all pixels in the lattice. γ is the regularization parameter controlling the relative influence on the solution from the image prior model as compared to the restoration error term influence.

III. Parameter Estimation

In this section, we establish a key relationship between a GGMRF and the generalized Gaussian (GG) distribution, and present a simple method based on this relationship to estimate p for any given GGMRF image.

An inspection of (3) suggests that direct estimation of p from an observed GGMRF $\mathbf{x}$ would be difficult. The distribution is highly non-linear in p and dependence on p is through the neighborhood structure of $\mathcal{C}$. The problem can be simplified by noting similarities between the conditional distribution of $\mathbf{x}$ in (3),

p	Image Name	p	Image Name
0.33	Garbage Can	1.12	Books
0.46	Mountains 1	1.27	Grass 1
0.53	Desktop	1.31	Leaves 3
0.53	Mountains 2	1.33	Bushes
0.55	Windows	1.39	Woodgrain
0.62	Wrinkled paper	1.45	Grass 3
0.63	Landscape 2	1.48	Concrete
0.64	Hallway	1.56	Carpet 2
0.65	Landscape 1	1.58	Cork
0.74	Linoleum	1.63	Carpet 1
0.80	Leaves 2	1.72	Dirt
0.84	Tile	1.73	Painted door
0.96	Block wall	1.74	Clouds 3
0.97	Clouds 4	1.87	Clouds 5
1.04	Clouds 1	1.92	Clouds 2
1.08	Brick	1.93	Cloth seat
1.10	Leaves 1	2.36	Grass 2

TABLE I

Estimated p values for a wide variety of texture and scene images when the first order GGMRF model is applied.

and the density function for a single, zero mean, GG random variable d

$$f_d(d;p) = \frac{Ap}{2\sigma\Gamma(\frac{1}{p})}\exp\left\{-\left[\frac{A|d|}{\sigma}\right]^p\right\} \quad (5)$$

These similarities suggest the following hypothesis:

Hypothesis. Let $d_{s,a}$ be the difference between nearest neighbor pixels s and a of a GGMRF,i.e. $d_{s,a} = x_s - x_a$, where a is restricted to be a neighbor in one direction (e.g. a is always the left nearest neighbor). Then (neglecting boundary cases) $d_{s,a}$ is distributed as i.i.d. generalized Gaussian $\forall s \in S$ and has the same shape parameter as the GGMRF.

Observations. When (3) is expressed in terms of pixel differences, $d_{s,a} = x_s - x_a$, and then factored, the joint density of $\mathbf{x}$ takes on the form of products of terms

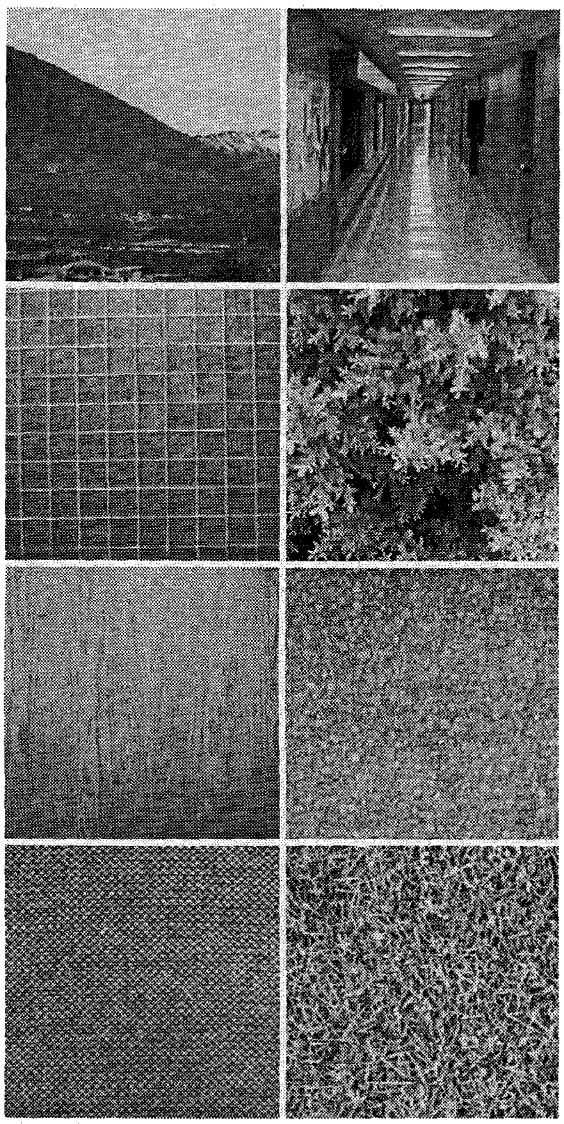

Fig. 2. Examples of GGMRF p value estimates for several texture and scene images. a) [top l.] "Mountains 1," $p = 0.46$; b) [top r.] "Hall," $p = 0.64$; c) [row 2 l.] "Tile," $p = 0.84$; d) [row 3 r.] "Leaves 1," $p = 1.10$; e) [row 3 l.] "Wood grain," $p = 1.39$; f) [row 3 r.] "Concrete," $p = 1.48$; g) [bot. l.] "Clouds 2," $p = 1.92$; h) [bot. r.] "Grass 2," $p = 2.36$.

which look like equation (5). This suggests the differences, $d_{s,a}$ are distributed generalized Gaussian. We also note that Besag argued similarly that the conditional distribution of a Gaussian Markov random field is Gaussian [5]. The hypothesis has also been confirmed experimentally over a wide range of p values by accurately estimating p for GGMRF's through $d_{s,a}$, using estimation methods designed for GG random variables. □

Given $d_{s,a}$ we can form a simple estimate for p based on kurtosis. It can be shown that the exact relationship between kurtosis and the GG shape parameter p is

$$\beta_2 = \frac{\Gamma(\frac{5}{p})\Gamma(\frac{1}{p})}{\left[\Gamma(\frac{3}{p})\right]^2}. \tag{6}$$

The sample kurtosis can be computed as

$$\hat{\beta}_2 = \frac{|S| \sum_{s\in S} (d_{s,a} - \bar{d})^4}{\left[\sum_{s\in S} (d_{s,a} - \bar{d})^2\right]^2}, \tag{7}$$

where a (as above) is the one directional nearest neighbor of s, $|S|$ is the cardinal number of the set of pixels on the lattice, and $\bar{d} = \frac{1}{|S|}\sum_{s\in S} d_{s,a}$. After an estimate of kurtosis is obtained, $\hat{p}$ is computed by solving equation (6). No closed form solution for p in known, however a table look-up approximate inversion of (6) is easily computed. In practice we have done this efficiently by sampling equation (6) for a number of values of p, and then using cubic spline interpolation between the nearest table entries to approximate the value of p that corresponds to $\hat{p}$. We call this the "inverse kurtosis method." Several authors have used kurtosis to estimate p for GG random data, but they have used only an approximate relationship and therefor have produced biased estimates [6] [7].

IV. An Iterative Adaptive Algorithm

The shape parameter estimator introduced above requires that the GGMRF, $\mathbf{x}$, be uncorrupted by blur or noise. The algorithm presented in this section enables us to apply these estimation methods even in the case of a corrupted GGMRF, and thus to jointly estimate $\mathbf{x}$ and p. The approach is similar to an Expectation-Maximization (EM) algorithm, and involves a bootstrap procedure which alternates between estimates of p and $\mathbf{x}$ until convergence is achieved.

Adaptive GGMRF Algorithm

1. Choose an initial shape parameter estimate, $\hat{p}^{(0)}$, and a image estimate, $\hat{\mathbf{x}}^{(0)}$, for the GGMRF prior model (e.g. $\hat{p}^{(0)} = 2.0$ and $\hat{\mathbf{x}}^{(0)} = \mathbf{y}$.)
2. Fix $p = \hat{p}^k$ and compute

$$\hat{\mathbf{x}}^{(k+1)} = \arg\{\min_{\mathbf{x}} \Phi(\hat{\mathbf{x}}^{(k)}, \mathbf{y}; p)\},$$

   where $\Phi(\mathbf{x}, \mathbf{y}; p)$ is the energy function of the GGMRF prior model as given in equation (4). Use e.g. Metropolis algorithm, Gibbs sampler, etc.
3. Using $\hat{\mathbf{x}}^{(k+1)}$, compute a new estimate $\hat{p}^{(k+1)}$ by forming the nearest neighbor difference image, $\mathbf{d}$ and solving equations (7) and (6).
4. If $\hat{p}^{(k+1)} \approx \hat{p}^{(k)}$, terminate, otherwise increment k and go to step 2.

The optimization called for in step 2 represents a conventional MAP restoration, and can be accomplished in a number of ways. We have used the Metropolis algorithm [8] [4], though other approaches such as the Gibbs Sampler should work as well.

V. Restoration Results

Our experiments have shown that the adaptive algorithm works well in estimating both $\mathbf{x}$ and p when $\mathbf{x}$ is truly a (synthetic) GGMRF and the observed image is corrupted by both blur and noise. Chen's algorithm [9] was used to generate GGMRF's for a variety of p values in the range of $.7 < p < 3$. These images were convolved with a 3 by 3 pixel uniform blur, and then i.i.d. Gaussian noise was added at 20 dB SNR. The corrupted images were restored using the adaptive GGMRF algorithm. Estimates of p were acceptably accurate (e.g. ± 0.2) and restoration error was better than that achieved using a conventional Gaussian Markov random field model (i.e. $p = 2$).

The more interesting question however is whether the algorithm performs well with more realistic images. The following experiment was designed to test the performance for more typical images, which are clearly not exactly modeled by a GGMRF. Two of the texture images in Figure 2, d) "Leaves 1," and g) "Cloth seat," were blurred with a 3 by 3 pixel averaging window, and i.i.d. Gaussian noise was added for an SNR of 20 dB. The corrupted images were restored using the adaptive GGMRF algorithm, with an initial guess of $p = 2.0$. The restored images (not shown) had significantly improved visual quality, and the joint estimates for p were well within an acceptable range. For "Leaves 1," $\hat{p} = 1.26$, (compared to the unblurred image estimate of $p = 1.10$.) For "Cloth seat," $\hat{p} = 1.45$, with an unblurred estimate of $p = 1.93$.

As another performance example, the 128-by-128 image shown in Figure 3a was blurred by a 25-by-1 PSF $= [1\ 1\ \cdots\ 1]$, representing a 1D horizontal motion blur. i.i.d. Gaussian noise at an SNR of 30 dB was added to the blurred image to produce figure 3b. The shape parameter estimated directly from the uncorrupted Figure 3a was 0.8.

The adaptive algorithm was applied to Figure 3b to jointly estimate $\mathbf{x}$ and p. Ten iterations were used to generate Figure 3c. The starting value of p was 2; the ending estimate was $\hat{p} = 0.61$. For comparison, a MAP restoration using a GMRF ($p = 2$) was computed and shown in Figure 3d. The squared error in Figure 3d is twice that of the error in Figure 3c. Though some of the blurring due to horizontal motion is reduced in Figure 3d, the result still looks over-smoothed. On the other hand, Figure 3c is both visually and numerically better because the edges were preserved as a result of adapting the model to the image.

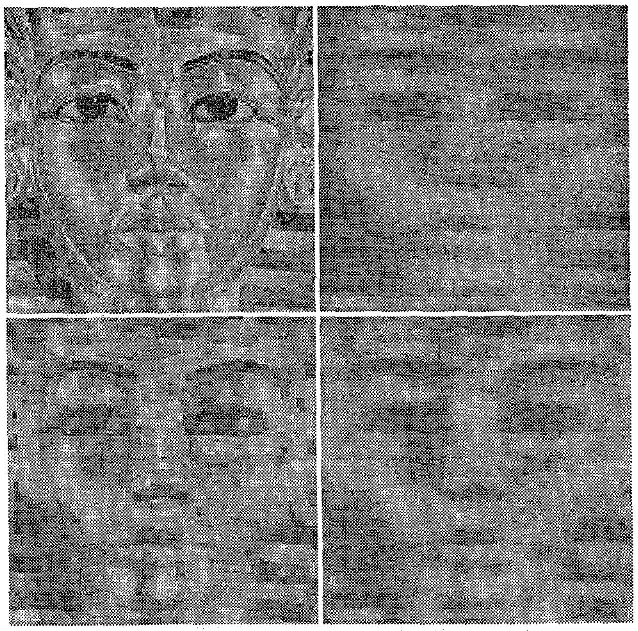

Fig. 3. Images from the experiment of the adaptive algorithm. a) [top l.] Original 128-by-128 image, b) [top r.] Blurred noisy image, c) [bot. l.] Adaptive GGMRF MAP restoration of a, d) [bot. r.] GMRF model restoration of a.

References

[1] C. Bouman and K. Sauer, "A generalized Gaussian image model for edge-preserving MAP estimation", *IEEE Transactions on Image Processing*, vol. 2, no. 3, pp. 296–310, July 1993.

[2] W. H. Pun and B. D. Jeffs, "Shape parameter estimation for generalized Gaussian Markov random field models used in MAP image restroation", in *Conference Record of the Twenty-Ninth Annual Asilomar Conference on Signals, Systems, and Computers*, Oct. 29–Nov. 1 1995.

[3] S. S. Saquib, C. A. Bouman, and K. Sauer, "Efficient ML estimation of the shape parameter for generalized Gaussian MRF", in *IEEE International Conference on Acoustics, Speech, and Signal Processing*, 1996, vol. 4, pp. 2227–2230.

[4] S. Geman and D. Geman, "Stochastic relaxation, Gibbs distributions, and the Bayesian restoration of images", *IEEE Transactions on Pattern Analysis and Machine Intelligence*, pp. 721–741, Nov. 1984.

[5] J. Besag, "Towards Bayesian image analysis", *Journal of Applied Statistics*, vol. 16, no. 3, pp. 395–407, 1989.

[6] A. H. Money, J. F. Affleck-Graves, M. L. Hart, and G. D. I. Barr, "The linear regression model: l_p-norm estimation and the choice of p", *Communications in Statistics - Simulation and Computation*, vol. 11, no. 1, pp. 89–109, 1982.

[7] V. A. Sposito and M. L. Hand, "On the efficiency of using the sample kurtosis in selecting optimal l_p estimators", *Communications in Statistics - Simulation and Computation*, vol. 12, no. 3, pp. 265–272, 1983.

[8] N. Metropolis, A. W. Rosenbluth, M. N. Rosenbluth, A. H. Teller, and E. Teller, "Equation of state calculations by fast computer machines", *Journal of Chemical Physics*, vol. 21, pp. 1087–1092, 1953.

[9] C. C. Chen, *Markov random field models in image analysis*, PhD thesis, Michigan State University, East Lansing, 1988.